MDPI

Article

Measurement of the Speed of Induction Motors Based on Vibration with a Smartphone

Paula Paramo-Balsa [1] , Juan Manuel Roldan-Fernandez [1,*] , Francisco Gonzalez-Longatt [2,*] and Manuel Burgos-Payan [1]

1   Department of Electrical Engineering, Escuela Técnica Superior de Ingeniería, Universidad de Sevilla, 41092 Sevilla, Spain; pparamo@us.es (P.P.-B.); mburgos@us.es (M.B.-P.)
2   Department of Electrical Engineering, Information Technology and Cybernetics, University of South-Eastern Norway, 3918 Porsgrunn, Norway
*   Correspondence: jmroldan@us.es (J.M.R.-F.); fglongatt@fglongatt.org (F.G.-L.)

Abstract: Induction motors are key pieces of equipment in today's society, powering a variety of industrial drives and home appliances. The induction motor speed is often used to monitor the performance of all kinds of industrial drives. For example, in the industrial field, the motor speed is very often used to determine the efficiency and mechanical load of motors. In this work, a new simple, low-cost, and nonintrusive procedure is proposed for infield measurement of induction motors speed, which is based on the spectral analysis of the vibration signal of the motors. The motor vibration signal is first acquired using the accelerometers integrated into a basic phone. The acquired signal is then treated by a MATLAB-based algorithm, which can determine the motor speed by identifying the mechanical frequency of the rotor shaft from the harmonic content of the vibration signal. In this way, it is shown that the mechanical frequency corresponding to the speed of rotation of the motors can be acquired by means of the embedded accelerometers of a common smartphone, avoiding the acquisition and installation of external accelerometers. To the authors' knowledge, this could be the first time that a smartphone has been proposed as a practical means of measuring the speed of a motor by analysing its vibration. Experimental results from an extensive set of tests, including the supply of the motor from a frequency converter, show that the speed can always be measured with a relative error of less than 0.15%.

Keywords: induction motors; vibration signature analysis; motor speed measurement; noninvasive motor speed measurement; infield motor speed measurement

1. Introduction

Electric motors are a fundamental part of the industrial and commercial equipment in society. They are used in a wide variety of industrial applications, as well as at the domestic consumer level in many household appliances. Induction motors are used in a multitude of electric drive applications due to their simplicity, robustness, and low price [1]. It is estimated that three-phase cage induction motors power about 90% of industrial drives [2,3].

In recent decades, due to the continuous increase in the cost of electricity and the concern for sustainable development, different ways have been investigated to reduce the world's electricity consumption, since induction motors account for about 68% of the global industrial energy consumption [4]. Recent works have estimated that the energy consumption of electric motors could be reduced by about 4% to 5% by simply using the best available motors [5,6].

Among the different techniques available to estimate the efficiency of an industrial induction motor, the rotational speed measurement is a simple and widely used one [7,8]. Appropriate measurement of the rotational speed of induction motors is a key factor in

monitoring the state of the motor system. Traditionally, sensors such as encoders and resolvers are used for continuous speed monitoring. They should be coupled to the motor shaft or installed in close proximity of the rotating element [9] to measure the speed. This type of sensor requires extra wiring, extra space, and regular maintenance [10]. Due to all these reasons, the use of these sensors involves additional costs [11]. However, if the speed of an industrial induction motor needs to be monitored or supervised a few times a day (i.e., every hour) or for a few days, portable tachometers, mostly optical, are commonly used [12]. This approach presents an acceptable combination of measurement precision and low cost. This type of measurement requires having a reflective adhesive sticker in the motor shaft. Unfortunately, sometimes for safety reasons [13], and other times because the motor is inside a casing, the shaft of the motor is not accessible [14,15]. In these cases, to put the reflective sticker on the shaft, it is necessary to stop the machine, which can result in additional costs for the industry.

For all these reasons, in recent years, researchers have been focused on developing new ways of measuring the motor speed by means of different types of sensors (image, sound, and vibrations, among others), not specifically designed for speed measurement.

The development of more accessible image sensors, cameras, and image processing techniques has brought new image-based methods as an alternative to conventional techniques. For example, a system for measuring induction motors speed using a low-cost image device is presented in [16]. The method requires a camera, and it is necessary to make a mark in the motor shaft. In [17], the speed of a motor is estimated using a tachometer based on a webcam. The authors proposed a method to estimate the relative load of three-phase induction motors for application in electrical energy audits. Methods based on images are nonintrusive, but the rotor shaft must be visible so that the camera can capture its movement.

Similarly, thanks to advances in low-cost sound sensors, sound-based methods to measure the rotational speed are a novel alternative. An algorithm that processes a sound signal emitted by an IM to estimate the speed, the torque, and the efficiency was introduced in [18]. The system was developed using an Arduino board and an analog microphone. The method is nonintrusive, but extra specific hardware is required, and it does not perform properly when induction motors are fed with frequency converters. In [19], a new low-cost and nonintrusive procedure is proposed for the field measurement of the speed of induction motors, which is based on the analysis of the spectrum of the audible noise emitted by the motors. A smartphone is used to acquire the motor noise. The noise signal is then processed by an algorithm based on MATLAB, which can establish the speed of the motor by identifying the frequency of the rotor shaft.

Other studies focused on the acquisition and analysis of motor currents for fault diagnosis purposes [20], and are also used to estimate the rotor speed [21–23]. The current of the stator is sampled and analysed to detect harmonic components that depend on the rotor speed. Such estimation techniques avoid the use of electromechanical sensors, which are usually expensive, fragile, and often difficult to install, but they still require some extra devices to capture and analyse these currents, which are not always accessible or easy to measure.

The interaction between the set of alternating currents that circulate through the windings and the electromagnetic fields that occur in an induction motor yields to the production of an electromagnetic torque on the motor shaft. However, that same interaction between electromagnetic fields and currents, combined with some physical anisotropy of the materials and some small mechanical manufacturing imperfections, also leads to the manifestation of undesirable radial and axial forces between the stator and the rotor of the motor. These undesired parasitic forces produce mechanical vibrations that are transmitted and spread throughout the entire motor housing and the whole attached mechanical structure. The amplitude of the vibrations at a point of the motor depends on both the strength of the forces and the mechanical response of the motor casing and its structure [7]. Vibrations analysis has been used for a long time and extensively as

an operational technique for motor condition monitoring [24,25]. But motor vibration incorporates a significant component that is excited by the mechanical rotation of the shaft. Consequently, vibration signal analysis has also been exploited to develop methods for measuring the motor speed [26].

The interest in this measurement principle continues today, as this technique provides good precision compared to other methods [7,27].

In [7], an experimental comparison between the estimation of the speed of an induction motor by means of the vibration signal and by the motor current signal was carried out. The work concluded that the speed of a motor fed with an inverter could be measured with an error lower than 0.05% using the vibration signal while applying different methods based on current analysis; the error always ranged between 0.4% and 0.6%. The most popular sensor for measuring rotational speed based on vibration is the accelerometer due to its precision [25,26]. The accelerometer measures the acceleration forces by means of a piezoelectric transducer, which transforms the mechanical strength into an electrical signal. Low-cost, easy-to-install, and accurate sensor alternatives are also explored. In [28], the performance of a magnetoresistive sensor is compared with a conventional accelerometer, concluding that although the first is a nonintrusive contactless method providing good results, in high magnetic field conditions, there is a risk of a disruption in vibration measurements. The possibility of using an electrostatic sensor to measure vibrations is analysed in [25]. Even though it is a low-cost candidate sensor, the results show that it captures unwanted noise because the electrode of the sensor is exposed to the air, which disrupts the vibration signal. As can be seen, there is still a need to investigate other possible sensors that allow motor vibrations to be measured with a nonintrusive, accurate, and low-cost method. This is where smartphones can play a relevant role.

Today, mobile technology continues to evolve rapidly thanks to the integration of faster multicore chips, memories with increasing sizes, and a growing number of refined sensors, each time more sophisticated. The large and growing number of smartphones (about four billion phones in 2021 [29]), the continuous performance improvement, and expansion of their features help to explain the current trend to use smartphones in a wide variety of applications, replacing or substituting other specific and conventional sensors. The use of embedded sensors in mobile phones offers important advantages, among which it is worth highlighting the ubiquity and low cost of the equipment and the ease of access and dissemination of information (data) thanks to its communication capabilities [30]. Smartphones have different sensors, such as photo and video cameras, microphones, GPSs, or accelerometers. The rich endowment of sensors integrated into cell phones presents the opportunity to use these appliances (gadgets) to develop sensors systems [31–33] suitable to monitor areas as different as the environment [34], traffic [35], or human health [36], among others.

Following this trend, this paper proposes and develops a new nonintrusive and infield method to measure the speed of induction motors, based on vibration spectral analysis, using a simple smartphone. To achieve that goal, the vibration signal is first acquired using a common smartphone. A free application [37], previously installed on the phone, is then used to access the information of the accelerometer built into the smartphone, creating a csv file with the information on the temporal evolution of the vibration in each of the three spatial directions. The vibration record (csv file) is sent wirelessly to the computer. Using a tailor-made routine developed in MATLAB, the csv file with the axial vibration records is loaded, and the frequency spectrum of the motor vibration is obtained. A peak detection algorithm leads to estimate the motor speed as corresponding to the frequency at which the maximum amplitude of the vibration spectrum occurs.

The proposed method is quite simple and very easy to use since the vibrations are available at any point of the motor frame or even on its bench or adjoining structure. Additionally, the method does not depend on the parameters of the motor or how it is fed. It is a nonintrusive contact method that can be used without altering the service of the motor and without extra measuring devices.

After this introduction, the rest of the document is organised as follows. Section 2 presents the theoretical background of the proposed method to measure rotor speed by spectral vibration signature analysis. Section 3 shows the main results of the set of tests carried out to prove the method. In Section 4, a short discussion of the proposed method is presented. To end, Section 5 summarises the most relevant conclusions of this research.

2. Materials and Methods

The complex vibration signal of a motor contains, among others, a component (of great amplitude) at the mechanical frequency of rotation of the rotor, which can be acquired and used to estimate the speed of rotation of the shaft. The mechanical frequency of rotation of the rotor can be obtained by applying to the frequency spectrum of the vibration signal a peak detection algorithm.

In this work, a new low-cost and nonintrusive method is proposed for the field measurement of the speed of induction motors. The method is based on the spectral analysis of motor vibration, but unlike other conventional techniques, the proposed method does not require the installation of any external accelerometer. The new proposal consists of acquiring the vibration signal by means of the accelerometers integrated in a common smartphone. The vibration signal is then processed by a MATLAB-based algorithm, which calculates the motor speed by recognising the mechanical frequency of the rotor shaft from the spectrum of the vibration signal. To the authors' knowledge, this is the first time that a smartphone is proposed as a practical means of motor speed measurement by motor vibration signature analysis.

The new method proposes to use the accelerometers embedded in a common smartphone as sensors to capture the vibration signal produced by an induction motor during its operation. A free application [37] was used to create a csv file with the time record of the axial components of the motor vibration signal, $f_{REF}(t)$, for each reference axis, $REF = \{X, Y, Z\}$. Finally, an algorithm based on MATLAB computes the rotation speed by finding the mechanical frequency of the rotor shaft from the harmonic spectrum of the vibration signal.

Figure 1a shows the educational test bench of the induction motor and the configuration of the different tests carried out in this work. As shown, the core of the test platform is the induction motor, whose vibrations are captured and registered by a common smartphone. A magnet and a self-adhesive magnet are required to fix the smartphone to the induction motor chassis, as shown in Figure 1b.
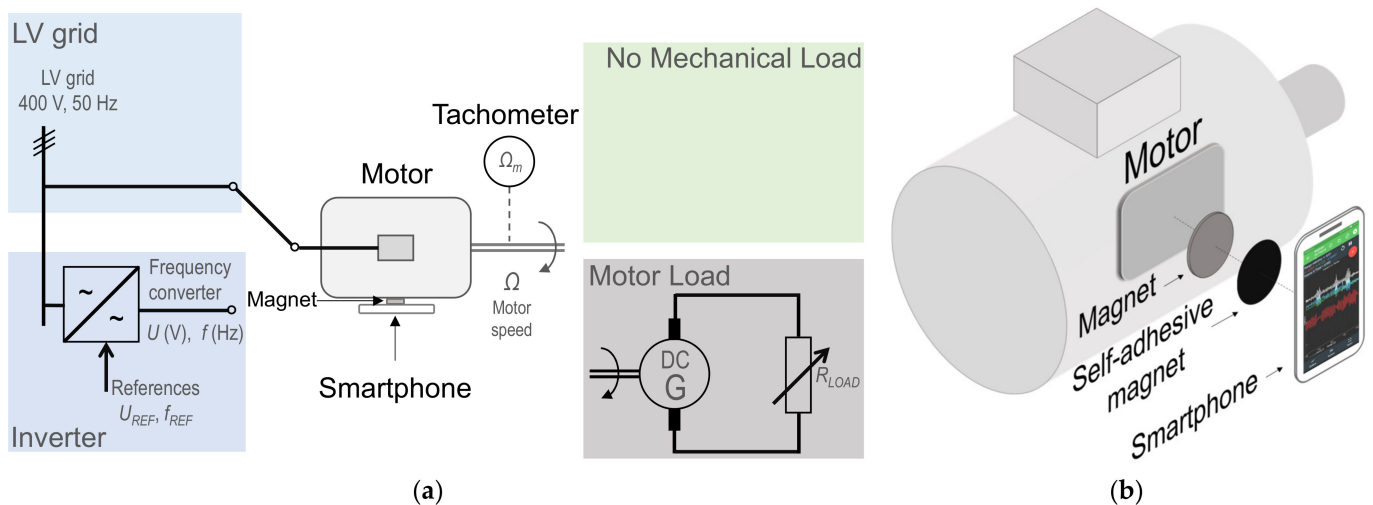

Figure 1. (**a**) Schematic of the different tests performed; (**b**) Scheme to show how the smartphone is attached to the induction motor during the tests by means of a self-adhesive magnet.

Two different power supplies were used: the grid supply and a frequency converter. The motor shaft can be left free, without mechanical load, or can be coupled to a DC

generator that supplies a variable resistance, allowing the load torque of the motor to be adjusted. During the tests, the rotation speed of the motor shaft was measured using a portable optical tachometer because it is a well-established and conventional contactless method. In all tests, the speed of the motor, Ω_m, was measured twice using two different portable optical tachometers. The mean value of the measurements of the two speeds was considered as the real value of the rotor speed. In addition, a smartphone was used to capture and record the motor vibration signal. Appendix A includes extra information about the tachometers, the smartphone, the free application used for recording, the attachment of magnets, and the test bench used in this work.

All tests followed the next procedure. Once the test configuration was set (grid or inverter as supply source and the type of mechanical load), the rotor speed was measured using two portable optical tachometers. Once the value of the rotor speed was measured, a smartphone was attached to the induction motor through a magnet, and the samples of the axial components of the motor vibration, $f_X(t)$, $f_Y(t)$, and $f_Z(t)$, were recorded with the help of the free application. Subsequently, the recorded csv file obtained by the free application with the information about vibrations was processed with a routine programmed in MATLAB designed to obtain the frequency spectra of the axial vibration signals, $F_X(j\cdot\omega)$, $F_Y(j\cdot\omega)$, and $F_Z(j\cdot\omega)$. This way, the frequency components referred to the motor reference frame, X, Y, and Z, were obtained. These axes were taken as the absolute reference frame in this work because the axes of the smartphone accelerometer, X', Y', and Z', change according to the relative position of the smartphone. For example, Figure 2a illustrates the selected reference frame, along with the axes of the smartphone accelerometer when the smartphone is perpendicular to the motor shaft and placed on the nameplate. In Figure 2b, the smartphone is parallel to the axis motor and over the terminal box.
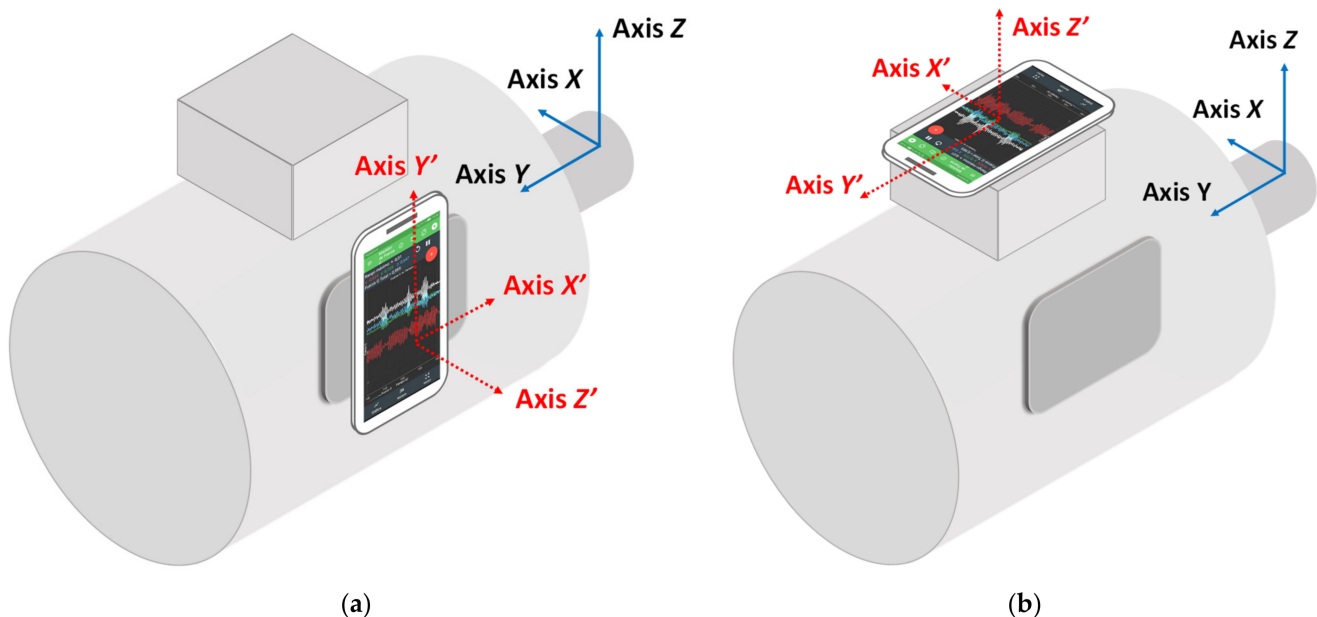

(**a**)　　　　　　　　　　　　　　　　(**b**)

Figure 2. Absolute reference frame considered in this work, X, Y, and Z, when the longitudinal axis, Y', of the smartphone is (**a**) perpendicular to the motor shaft and on the nameplate and (**b**) parallel to the motor shaft and over the terminal box.

The frequency spectrum of the components of the motor vibration signal for each reference axis was obtained using the Fourier transform

$$F_{REF}(j\cdot\omega) = \int_0^{(N-1)\cdot T} f_{REF}(t)\cdot e^{-j\cdot\omega}\cdot dt \tag{1}$$

where $F_{REF}(j \cdot \omega)$ represents the set of Fourier transforms (frequency domain) of the functions of time, $f_{REF}(t)$, corresponding to each reference axis, *REF = {X, Y, Z}*, *N* represents the number of samples (through which the time signal has been acquired), and T is the uniform sampling period. The continuous Fourier transform (1) is approximated by the discrete Fourier transform (DFT) when the signals are known only at a few instants separated by sampling times. The DFT was obtained by means of the fast Fourier transform algorithm. The fast Fourier transform (FFT) algorithm was used because it calculates the discrete Fourier transform taking advantage of symmetry and periodicity of the signal, what reduces its computational cost [38]. After obtaining the Fourier transform of the motor vibration signal for each reference axis, $F_X(j \cdot \omega)$, $F_Y(j \cdot \omega)$, and $F_Z(j \cdot \omega)$, the root mean square (RMS) value of the vibration spectrum, $|F(j \cdot \omega)|$, was obtained as

$$|F(j \cdot \omega)| = \sqrt{\sum_{REF=\{X,Y,Z\}} |F_{REF}(j \cdot \omega)|^2} = \sqrt{|F_X(j \cdot \omega)|^2 + |F_Y(j \cdot \omega)|^2 + |F_Z(j \cdot \omega)|^2} \quad (2)$$

A MATLAB-based algorithm calculated the fundamental mechanical frequency of the rotor shaft, ω_F, simply by applying a peak detection algorithm to the RMS vibration spectrum

$$\omega_F : \ |F(j \cdot \omega_F)| = \mathrm{MAX}|F(j \cdot \omega)| \quad (3)$$

Finally, the motor speed value, Ω, was calculated as

$$\Omega = 2 \cdot \pi \cdot \omega_F \quad (4)$$

The value of the absolute relative error of the result was calculated comparing the estimation speed obtained using vibrations, Ω, with the actual rotor speed measured with two tachometers, Ω_m

$$\varepsilon = \left| \frac{\Omega - \Omega_m}{\Omega_m} \right| \quad (5)$$

The flow chart in Figure 3 presents an overview of the proposed procedure to estimate the rotation speed of the motor shaft.
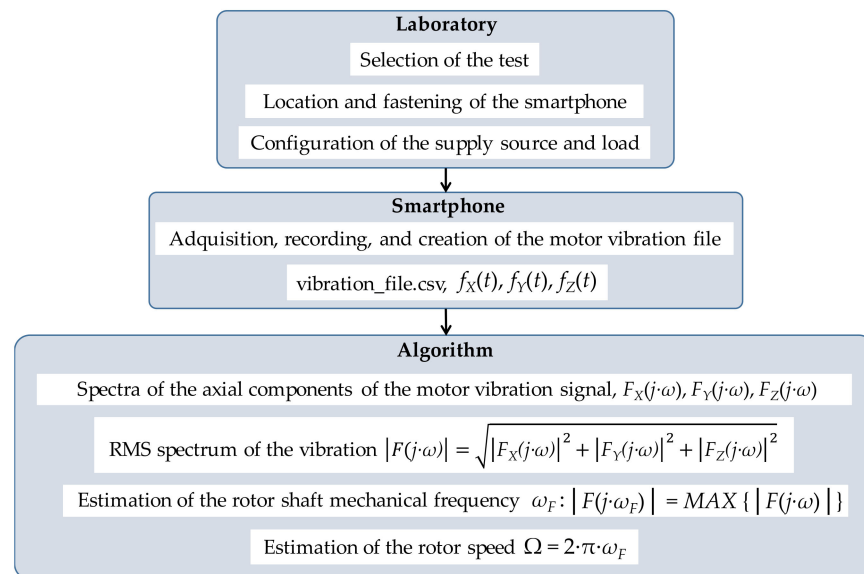

Figure 3. Flow diagram of the proposed method to estimate the rotational speed based on the vibration.

Speed Estimation Method

In order to better illustrate the proposed methodology, an example will be described step-by-step. A sample vibration recording corresponding to a two-pole induction motor fed from the supply mains, at no load (no mechanical load attached to the motor shaft), will be used as a case example. The average value of rotational speed measured by tachometers is Ω_m = 2820 r/min, or in other words, a shaft mechanical rotation frequency of ω_m = 47 Hz. Figure 4 shows the axial components of the time motor vibration, $f_X(t)$, $f_Y(t)$, and $f_Z(t)$, obtained from the csv file recorded by means of the free application. Figure 5 shows the spectra of the components of the motor vibration signal, $|F_X(j \cdot \omega)|$, $|F_Y(j \cdot \omega)|$, and $|F_Z(j \cdot \omega)|$, obtained by the MATLAB-based routine. Finally, Figure 6 shows the RMS spectrum of the motor vibration, $|F(j \cdot \omega)|$, computed by means of (2).
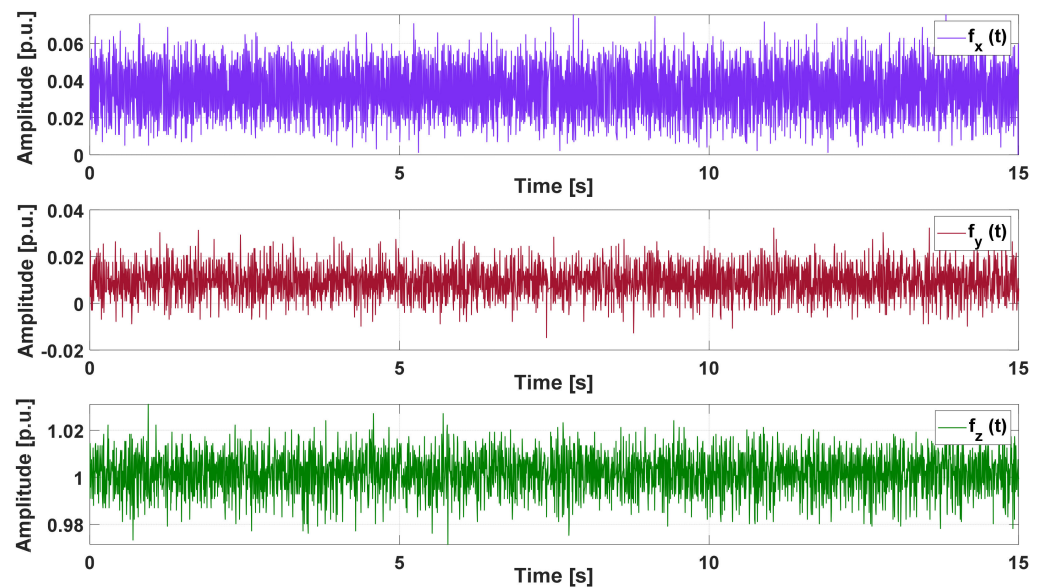
Figure 4. Time vibration signal of the motor fed from the supply mains, at no load (no mechanical load), at 2820 r/min for axis x (**top**), y (**middle**), and z (**bottom**).

Next, a peak detection routine was used to determine the highest peak of the RMS spectrum of the motor vibration, $|F(\omega_F)| = MAX\{|F(\omega)|\}$. Accordingly, the proposed algorithm determined the rotor shaft mechanical frequency, ω_F, as the frequency corresponding to the highest magnitude of the RMS spectrum, that is, $|F(\omega_F)| = MAX\{|F(\omega)|\}$. In the example of Figure 6, the RMS spectrum of the motor vibration reached its maximum at a rotor shaft mechanical frequency of ω_F = 47.0215 Hz ($|F(\omega_F = 47.0215 \text{ Hz})| = MAX\{|F(\omega)|\}$ = 23.8414 p.u.). Finally, using (4), the estimation rotor speed was Ω = 2821.29 r/min. The relative error of the estimation, compared to the measured value obtained using the tachometers (Ω_m = 2820 r/min), was ε = 0.0457%, demonstrating very good agreement.
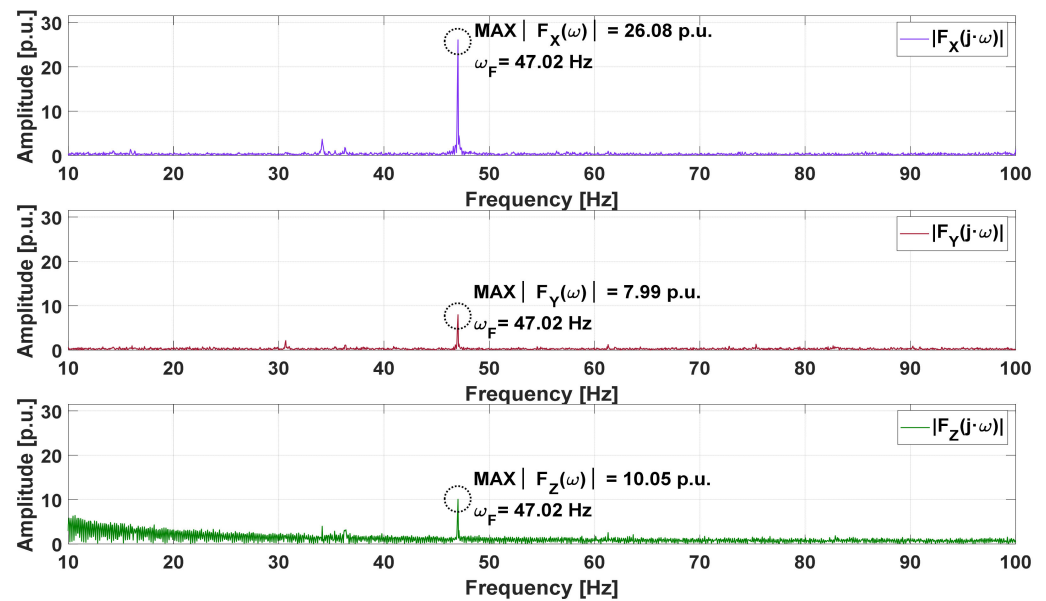
Figure 5. Frequency spectra of the components of the vibration signal corresponding to the motor fed from the supply mains, at no load (no mechanical load), at 2820 r/min for axis x (**top**), y (**middle**), and z (**bottom**).
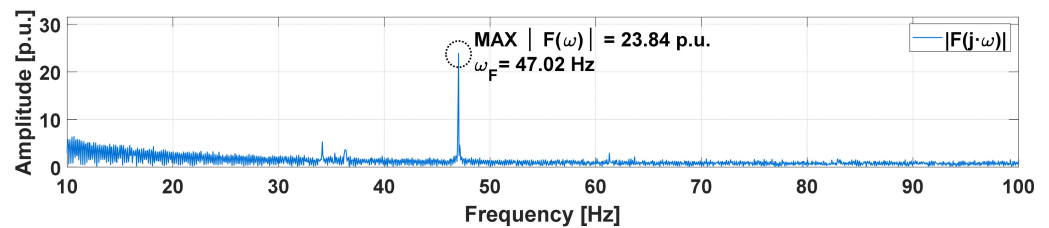

Figure 6. RMS frequency spectrum of the vibration signal of the motor fed from the grid, for no load (free motor shaft) at 2820 r/min.

3. Results

This section contains the experimental results of the tests carried out to demonstrate the effectiveness of the proposed method for measuring motor speed. It is important to note that all tests were carried out on an educational test bench. Different machines, structures, and portable measuring instruments were placed over the common surface. This means that devices on top common surface could generate extra vibrations.

The configurations (source and load, Figure 1) of the test were as follows:

- Feeding source
  - Supply grid (400 V, 50 Hz)
  - Frequency converter or inverter, which allows adjusting voltage and frequency values of the motor power supply
- Mechanical load
  - No mechanical load (free motor shaft)
  - DC generator feeding a variable resistive load

As shown in Figure 7, three smartphone locations were considered during the tests. The smartphone was placed over the terminal box in *Pos1*, over the nameplate in *Pos2*, and on the support bench in *Pos3*. Furthermore, different recording times (5, 10, and 15 s) and sets of magnets (Figure 7) were tested to prove the robustness and precision of the developed method, regardless of the different implementation parameters.
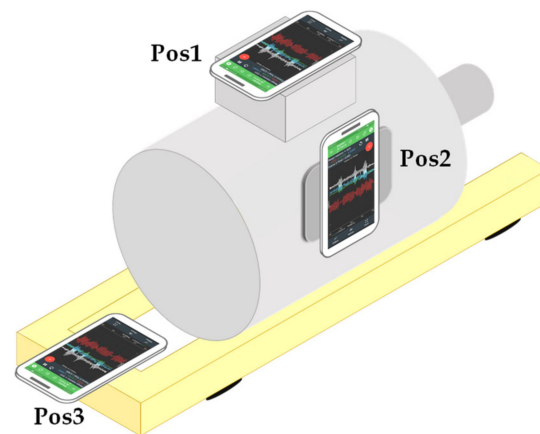
Figure 7. Smartphone locations for the different tests.

Nevertheless, the recordings reported in this work correspond mainly to the smartphone in *Pos1*, fixed with a magnet (support) of 40 mm diameter, recordings of t = 10 s length, and a sampling frequency, ω_s = 200 Hz.

3.1. Motor Supply from Mains with a DC Generator as Variable Mechanical Load

In this configuration, a two-pole induction motor was directly fed from the supply mains at 400 V, 50 Hz. The motor shaft was mechanically coupled to the rotor of a DC generator. The armature of the DC generator was used to feed a resistance, variable at steps, which allowed the adjustment of the mechanical load torque and, consequently, the speed of the induction motor. The available resistance assembly allowed the rotor speed to vary from 2857 r/min (47.62 Hz) to 2990 r/min (49.83 Hz). Figure 8a shows the setup of the tests, and Figure 8b shows eight RMS spectra of the vibration signals of the motor, $|F(j \cdot \omega)|$, for the indicated range of rotor speeds.
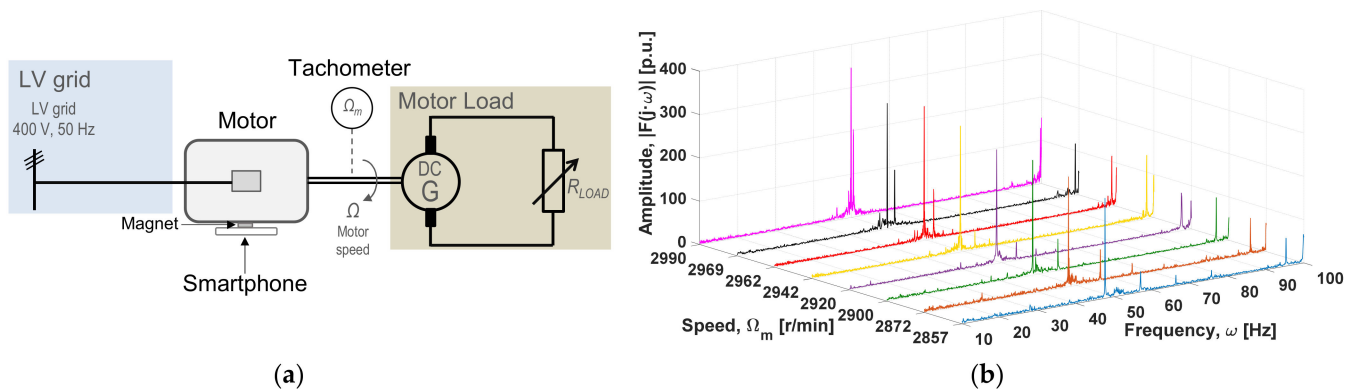
Figure 8. Motor fed from the mains at 400 V, 50 Hz, and a coupled DC generator: (**a**) test setup; (**b**) RMS spectra of vibration signals for motor speeds ranging from 2857 r/min to 2990 r/min.

Table 1 summarises the results for each value of the load resistance, R0–R7. The second and third columns shown, respectively, the actual values of the rotor speed, Ω_m, and the corresponding mechanical frequency of the mechanical frequency of the rotor shaft, ω_m, calculated from (4). Additionally, the rotor speed, Ω, and rotor shaft frequency, ω_F, both obtained by the algorithm, are shown in the fourth and fifth columns. Finally, the relative errors, ε, are calculated in the sixth column. As can be seen, the relative errors are very small. Indeed, in the worst case, the relative error is under 0.09%.

Table 1. Motor fed from the mains at 400 V, 50 Hz, and coupled to a DC generator. Measured and calculated values of rotor speed and frequencies, as well as relative errors.

Resistance	Experimental		Algorithm		Relative Error
	Ω_m (r/min)	ω_m (Hz)	Ω (r/min)	ω_F (Hz)	ε (%)
R7	2857	47.62	2859.4	47.66	0.0831
R6	2872	47.87	2871.1	47.85	0.0316
R5	2900	48.33	2900.4	48.34	0.0135
R4	2920	48.67	2920.9	48.68	0.0308
R3	2942	49.03	2941.4	49.02	0.0202
R2	2962	49.37	2961.9	49.37	0.0029
R1	2969	49.48	2970.7	49.51	0.0574
R0	2990	49.83	2991.2	49.85	0.0405

Table 2 shows the relative errors in the estimation of the rotor speed for different time recordings of 5, 10, and 15 s and different locations of the smartphone on top of the motor (*Pos1*, *Pos2*, and *Pos3*, see Figure 7). In general terms, although *Pos1* with longer recordings (15 s) often led to the better speed estimation, the error always remained rather low, ranging from 0.0131% to 0.1311%.

Table 2. Motor fed from the mains at 400 V, 50 Hz, and a DC generator coupled to the motor shaft. Relative errors corresponding to different smartphone positions and different values of the resistance load and time recording length.

Resistance	Time Recording (s)	Relative Error, ε (%)		
		Smartphone Locations over the Motor		
		Pos1	*Pos2*	*Pos3*
R7	5	0.1130	0.0831	0.0131
	10	0.1130	0.0831	0.0131
	15	0.0106	0.0194	0.0131
R4	5	0.0696	0.0696	0.0626
	10	0.1311	0.0308	0.0626
	15	0.0308	0.0308	0.0377
R1	5	0.0911	0.0574	0.0237
	10	0.0911	0.0574	0.0237
	15	0.0911	0.0574	0.0237

The results in Table 2 prove that changes in the position of the smartphone or the length of time recordings do not seriously affect the estimations of the rotor speed since the relative errors are similar.

3.2. Motor Fed from a Inverter Coupled to a DC Generator

In this configuration, a frequency converter was used to power the induction motor at frequencies from 30 Hz to 80 Hz. The motor shaft was coupled to a DC generator, feeding an adjustable resistance, acting as variable mechanical load for the motor. Figure 9a shows the test sketch, and Figure 9b shows six RMS spectra of the vibration signals, $|F(j \cdot \omega)|$, when the IM was fed at 400 V 45 Hz by the converter corresponding to the rotor speeds from 2369 r/min to 2673 r/min.
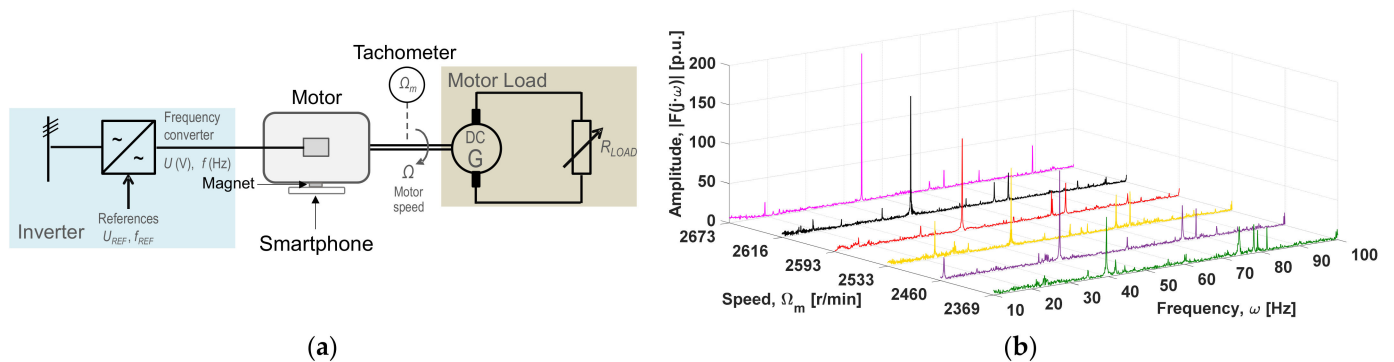
(**a**)

(**b**)

Figure 9. Motor fed from a frequency converter (inverter) and driving a DC generator: (**a**) sketches of the test; (**b**) RMS spectra of vibration signals for rotor speeds ranging from 2369 r/min to 2673 r/min.

Table 3 shows the results of the measured rotor speeds for frequencies of the power supply ranging from 30 Hz to 80 Hz for various mechanical loads of the motor. For each frequency, as the mechanical load decreased (R7→R0), the rotor speed increased, as expected.

Table 3. Motor fed from a frequency converter, driving a DC generator. Values of speed measured (tachometer) for different values of resistance and the corresponding rotor speed estimations *.

Frequency Supplied (Hz)	Ω_1 ** (r/min)	Ω_m (r/min)							
		R7	**R6**	**R5**	**R4**	**R3**	**R2**	**R1**	**R0**
30.00	1800	1464	1490	1581	1640	1681	1722	1739	1779
35.00	2100	1621	1701	1815	1885	1960	2016	2025	2074
45.00	2700			2369	2460	2533	2593	2616	2673
60.00	3600					3220	3400	3451	3564
70.00	4200						3790	3922	4142
80.00	4800							4243	4700

* Values not reported correspond to cases out of the converter capability. ** Ω_1 is the synchronous speed for the supply frequency.

Tables 4–6 summarise the results for 35 Hz, 60 Hz, and 70 Hz, respectively. Although a full set of vibration recordings was made in all the cases reported in Table 3 (including other frequencies, several positions of the smartphone, and various recording time durations), only the results corresponding to 35 Hz, 60 Hz, and 70 Hz were selected to be shown in this section to illustrate the quality of the experimental results. Each of these tables shows the measured rotor speed, Ω_m, the rotor shaft frequency, ω_m, the estimated rotor speed, Ω, the estimated rotor shaft frequency, ω_F, and finally, the relative errors.

Table 4. Motor fed from a frequency converter, driving a DC generator. Measured and estimated values of rotor speed and frequencies, as well as relative errors at a frequency supply of 35 Hz.

Resistance	Experimental		Algorithm		Relative Error
	Ω_m (r/min)	ω_m (Hz)	Ω (r/min)	ω_F (Hz)	ε (%)
R7	1621	27.02	1620.1	27.00	0.0545
R6	1701	28.35	1702.1	28.37	0.0675
R5	1815	30.25	1816.4	30.27	0.0775
R4	1885	31.42	1886.7	31.45	0.0912
R3	1960	32.67	1962.9	32.71	0.1475
R2	2016	33.60	2015.6	33.59	0.0186
R1	2025	33.75	2024.4	33.74	0.0289
R0	2074	34.57	2074.2	34.57	0.0105

Table 5. Motor fed from a frequency converter, driving a DC generator. Measured and estimated values of rotor speed and frequencies, as well as relative errors at a frequency supply of 60 Hz *.

Resistance *	Experimental		Algorithm		Relative Error
	Ω_m (r/min)	ω_m (Hz)	Ω (r/min)	ω_F (Hz)	ε (%)
R3	3220	53.67	3222.7	53.71	0.0825
R2	3400	56.67	3401.4	56.69	0.0402
R1	3451	57.52	3451.2	57.52	0.0050
R0	3564	59.40	3562.5	59.38	0.0421

* The capability of the converter is exceeded for the cases corresponding to R4-R7.

Table 6. Motor fed from a frequency converter, driving a DC generator. Measured and estimated values of rotor speed and frequencies, as well as relative errors at a frequency supply of 70 Hz *.

Resistance *	Experimental		Algorithm		Relative Error
	Ω_m (r/min)	ω_m (Hz)	Ω (r/min)	ω_F (Hz)	ε (%)
R2	3790	63.17	3791.0	63.18	0.0268
R1	3922	65.37	3925.8	65.43	0.0964
R0	4142	69.03	4139.6	68.99	0.0568

* The capability of the converter is exceeded for the cases corresponding to R3-R7.

As can be seen in Tables 4–6, the obtained accuracy of the estimations when an inverter is used as a power supply is similar to the case when the motor is fed from the grid. The relative error always remained below 0.15%.

4. Discussion

The rather basic, low-featured smartphone used in this work only allowed the sampling of the axial components of the motor vibration with a maximum rate of 200 samples per second, that is, with a sampling frequency of ω_S = 200 Hz (as a reference, in [26], the vibration signal acquired from an external accelerometer, was sampled at 10 kHz). Consequently, the Nyquist–Shannon sampling theorem limits to ω_{F_MAX} = 100 Hz, the maximum value of the theoretical rotor shaft mechanical frequency that could be measured by the proposed method. In fact, the practical limit will be somewhat less than that theoretical value. Fortunately, this limitation is of little practical importance since industrial induction motors, for various considerations, are rarely operated at such high speeds. In a real case, this limitation would only affect two-pole motors, operating near twice the rated frequency (50–60 Hz), which is not very common in the industrial field. The synchronous speed of a four, six, or eight8-pole motor is 1/2, 1/3, or 1/4 times less than the synchronous speed of a two-pole motor, so the mechanical rotation frequency of the rotor will not exceed the maximum limit of the accelerometer built into the smartphone. Anyway, in case it was necessary to measure the speed of motors with higher rotor mechanical frequencies, it would be necessary to use a smartphone that allows acquiring the components of the motor vibration with a higher sampling frequency. Today's smartphones allow sampling frequencies of 400–500 Hz.

To compare the performance of the proposed methodology, Table 7 shows the results reported in [26], corresponding to three different two-pole induction motors fed from the grid (380 V, 50 Hz), whose speeds are estimated at no load and at full load by means of an external accelerometer sampled at 10 kHz (10 s duration). As can be seen, the errors ranged from 0.07% to 0.55%.

Table 7. Motor speed estimation with the motor fed from the mains (380 V, 50 Hz). Vibration signal sampled at 10 kHz for 10 s. Results from [26].

Motor Rated Power	Measurement			Estimate	Error
	Load Condition	Ω_m (r/min)	ω_m (Hz)	Ω (r/min)	ε (%)
15 kW	No load	1502.3	25.01	1500.62	0.11
	Full load	1454.0	24.37	1461.97	0.55
11 kW	No load	1498.0	24.95	1496.98	0.07
	Full load	1463.0	24.41	1464.36	0.09
3 kW	No load	1491.0	24.82	1489.08	0.13
	Full load	1396.0	23.20	1392.20	0.27

The results in Table 1 show that, with the proposed methodology, when the smartphone is placed in *Pos1* (vibration signal sampled at 200 Hz for 10 s) the relative errors are always under 0.09% (ranging from 0.0029% to 0.0831%), while Table 2 shows that for other smartphone positions and sample durations, the maximum error is lower than 0.14% (from 0.0131% to 0.1311%). As can be seen, the errors resulting from the proposed method based on the use of the accelerometer built-in the smartphone can be compared favourably with those reported in [26], in which an external accelerometer sampled at 10 kHz was used.

As it has been pointed out, the proposed method determines the motor speed by means of the frequency corresponding to the rotation of the mechanical shaft of the motor. But the method did not require the use of features unique to induction motors. Accordingly, although the tests were carried out with an induction motor, the proposed method should also be able to measure the speed of other kinds of electric machines and rotating devices.

The success of the proposed method relies on the premise that the frequency corresponding to the highest peak of the RMS value of the vibration signal spectrum, ω_F, matches the fundamental (first harmonic) of the rotor mechanical frequency. In a very low percentage (less than 3%) of the about 450 vibration signal samples analysed, and mainly related to the use of the converter, the frequency corresponding to the peak of the RMS value of the vibration signal spectrum corresponds to a frequency that does not match the mechanical frequency of the rotor shaft. In these scarce cases, the identification hypothesis is not fulfilled, and the rotor speed is not properly estimated.

An alternative extended method that allows treating even these very infrequent or exceptional cases is then proposed. The extended method only requires the analysis of the spectra of the vibration signals, $F_{REF}(\omega)$, corresponding to each reference axis, $REF = \{X, Y, Z\}$, and the identification of the frequencies corresponding to the peak of the three axial vibration signal spectra, ω_{F_REF}: $|F_{REF}(\omega_{F\_REF})| = \text{MAX}\{|F_{REF}(\omega)|\}$. That is, the highest amplitude frequency peak for each axis.

Extended Method

The extended method only requires the analysis of the spectra of the vibration signals, $F_{REF}(\omega)$, corresponding to each reference axis, $REF = \{X, Y, Z\}$. The mechanical frequency of the rotor, ω_F, is now identified as the frequency, ω_{F_REF}, corresponding to the maximum of the peaks of the amplitudes of the three axial vibration signal spectra

$$\omega_F = \omega_{F-REF} : |F_{REF}(\omega_{F-REF})| = MAX|F_{REF}(\omega)|, \ REF = \{X, Y, Z\}. \tag{6}$$

Finally, the rotor speed, Ω, was calculated by means of (4) as previously. Figure 10 summarises the flow chart of the extended method.
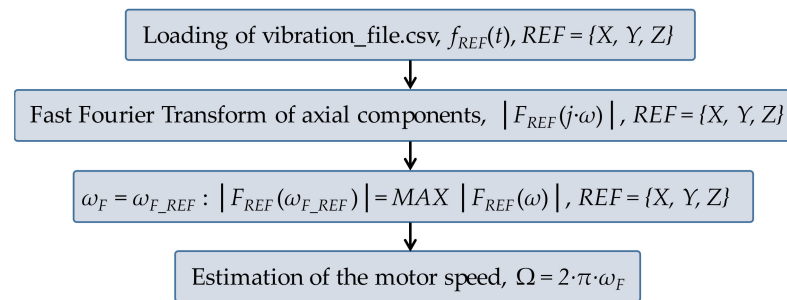
Figure 10. Flow chart of the extended method.

As an example of the application of the extended method, a recording of the axial components of the motor vibration was analysed step by step. The case corresponds to a motor speed of $\Omega_m = 1581$ r/min ($\omega_m = 26.35$ Hz).

As can be seen in Figure 11, the RMS value of the vibration spectrum shows a peak value of $|F_{MAX}(\omega)| = \text{MAX}\{|F(\omega)|\} = |F(\omega_{F\_RMS} = 73.8770 \text{ Hz})| = 93.2191$ p.u., which is placed at a frequency of $\omega_{F\_RMS} = 73.8770$ Hz. This is one of the rare cases where, using (3), the frequency corresponding to the highest peak of the RMS value of the spectrum does not match the mechanical frequency of the rotor shaft, $\omega_{F\_RMS} = 73.8770 \text{ Hz} \neq \omega_m = 26.35$ Hz.
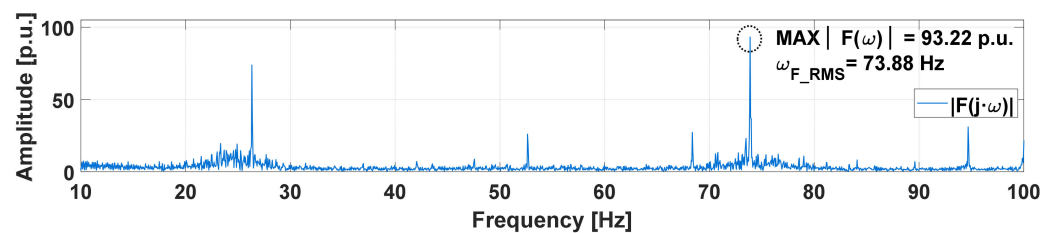

Figure 11. Frequency spectrum of the RMS value of the motor vibration at a rotor speed of $\Omega_m = 1581$ r/min ($\omega_m = 26.35$ Hz).

On the other hand, Figure 12 and Table 8 show that the peak value of the amplitude of the *X* component of the vibration signal spectrum is $|F_{X\_MAX}(\omega)| = \text{MAX}\{|F_X(\omega)|\} = |F_X(\omega_{F\_X} = 26.3184 \text{ Hz})| = 84.3203$ p.u. Figure 12 and Table 8 also show that the maximum peak value of the amplitudes of the three axial vibration signal spectra corresponds to the X axis since, $|F_X(\omega_{F\_X} = 26.3184 \text{ Hz})| = 84.3203$ p.u. $= \text{MAX}\{|F_{X\_MAX}(\omega)| = 84.3203$ p.u., $|F_{Y\_MAX}(\omega)| = 55.0815$ p.u., and $|F_{Z\_MAX}(\omega)| = 69.0521$ p.u.$\} = 84.3203$ p.u. That maximum peak takes place at $\omega_{F\_X} = 26.3184$ Hz. As a result, and according to (6), the mechanical frequency is taken as $\omega_F = \omega_{F\_X} = 26.3184$ Hz. Finally, using (4), the motor speed results in $\Omega = 1579.10$ r/min, which agrees with the tachometers ($\varepsilon = 0.1199\%$).

As can be seen, the extended method, using the same data source (the spectrum of the axial components of the motor vibration), is able to circumvent the difficulties in the identification of the mechanical frequency that occurs when using the RMS value of the vibration spectrum, leading to a proper calculation of the motor speed.
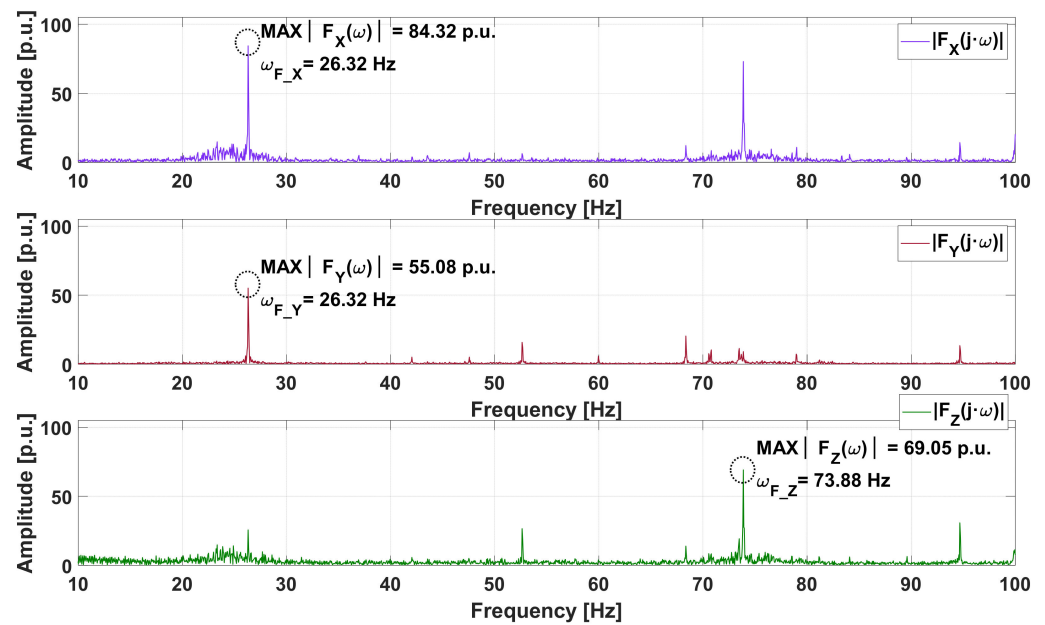
Figure 12. Spectra of the axial components of the vibration signal corresponding to a motor speed of $\Omega_m = 1581$ r/min ($\omega_m = 26.35$ Hz) for axis x (**top**), y (**middle**), and z (**bottom**).

Table 8. Peak values of the amplitude of the axial (upper part) an RMS (lower part) vibration signal spectra and corresponding frequencies.

Vibration Component Axis	Peak Value of the Amplitude of the Axial Vibration Signal Spectra, $|F_{REF}(\omega_{F\_REF})| = \text{MAX}\{|F_{REF}(\omega)|\}$	Frequency Corresponding to the Peak Value of the Amplitude of the Axial Vibration Signal Spectra, $\omega_{F\_REF}: |F_{REF}(\omega_{F\_REF})| = \text{MAX}\{|F_{REF}(\omega)|\}$
X	$\text{MAX}\{|F_X(\omega)|\} = |F_X(\omega_{F\_X} = 26.3184 \text{ Hz})| = 84.3203$ p.u.	$\omega_{F\_X} = 26.3184$ Hz
Y	$\text{MAX}\{|F_Y(\omega)|\} = |F_Y(\omega_{F\_Y} = 26.3184 \text{ Hz})| = 55.0815$ p.u.	$\omega_{F\_Y} = 26.3184$ Hz
Z	$\text{MAX}\{|F_Z(\omega)|\} = |F_Z(\omega_{F\_Z} = 73.8770 \text{ Hz})| = 69.0521$ p.u.	$\omega_{F\_Z} = 73.8770$ Hz
Vibration Component	Peak Value of the Amplitude of the RMS Vibration Signal Spectra, $|F(\omega_{F\_RMS})| = \text{MAX}\{|F(\omega)|\}$	Frequency Corresponding to the Peak Value of the Amplitude of the RMS Vibration Signal Spectra, $\omega_{F\_RMS}: |F(\omega_{F\_RMS})| = \text{MAX}\{|F(\omega)|\}$
RMS	$\text{MAX}\{|F(\omega)|\} = |F(\omega_{F\_RMS} = 73.8770 \text{ Hz})| = 93.2191$ p.u.	$\omega_{F\_RMS} = 73.8770$ Hz

5. Conclusions

This paper presents a new, simple, and nonintrusive method for inservice and field motor speed measurement, based on a smartphone as the acquisition and recording device of the vibration signal, and a MATLAB algorithm to determine the motor speed. The proposed method to measure the motor speed relies on the assessment of the frequency spectrum of the vibration data of the motor. In the experimental section, a sampling frequency as reduced as 200 Hz was sufficient for acquiring the necessary frequency components to determine the speed of a four-pole induction motor. This new method does not require the installation of any external accelerometer or other type of sensor, since the vibration signal is acquired by the accelerometers integrated into a common smartphone by means of a free application. Still, the proposed approach is a contact method. A magnet and a self-adhesive magnet are required to fix the smartphone to the induction motor chassis. These elements were chosen as a low-cost solution in the marketplace. The use of the accelerometer integrated into a smartphone allows avoiding the necessity of extra

space, extra wiring, regular maintenance, or accessibility of the rotor shaft. In addition, the proposed procedure does not require stopping the machine, unless strictly required for personal protection or security reasons.

The method was tested in the laboratory, feeding the motor with different power supplies (mains and inverter) and mechanical loads (no mechanical load and DC generator). An extensive set of tests was carried out in the laboratory, including different length (duration) of vibration samples and different positions/orientations of the smartphone on the tested motor, including the supporting frame.

Given that the proposed method is based on the identification of the frequency corresponding to the rotation of the mechanical shaft of the motor (without using features unique to induction motors), everything seems to indicate that it could also be used to measure the speed of any kind of rotating shaft device, although that feature was not tested in this work. The proposed method could also be adapted for near-real-time applications by means of a dedicated application.

In general terms, the motor speed estimation values obtained with the proposed method agree with the experimental results, proving that the method is accurate, versatile, and robust. The new method allows the motor speed to be measured with a relative error of consistently less than 0.15% in the worst of the analysed case. Consequently, the new method could be accepted as a new procedure to be included in the toolbox of established techniques for measuring the speed of induction motors.

Author Contributions: Conceptualisation, J.M.R.-F., P.P.-B., F.G.-L. and M.B.-P.; data curation, P.P.-B.; methodology, M.B.-P., P.P.-B. and J.M.R.-F.; validation, P.P.-B. and J.M.R.-F.; formal analysis, J.M.R.-F., P.P.-B. and M.B.-P.; investigation, J.M.R.-F., P.P.-B. and M.B.-P.; resources, P.P.-B. and F.G.-L.; software J.M.R.-F., P.P.-B. and F.G.-L.; writing—original draft, J.M.R.-F., P.P.-B. and M.B.-P.; writing—review and editing, M.B.-P., J.M.R.-F., P.P.-B. and F.G.-L.; visualisation, M.B.-P., P.P.-B. and J.M.R.-F.; supervision, J.M.R.-F., M.B.-P. and F.G.-L.; project administration and funding acquisition, F.G.-L. All authors have read and agreed to the published version of the manuscript.

Institutional Review Board Statement: Not applicable.

Informed Consent Statement: Not applicable.

Data Availability Statement: The data used for the manuscript are available on request.

Conflicts of Interest: The authors declare no conflict of interest.

Appendix A

Tables A1–A4 summarise, respectively, the main technical characteristics of the tachometers, induction motor, direct current generator, and frequency converter used in the experimental section of this work.

Table A1. Portable tachometers.

Tachometer	Tachometer 1	Tachometer 2
Number of digits	5	5
Range	2.5 to 99,999 r/min	5 to 99,999 r/min
Precision	±0.051% + 1 digit	±0.050% + 1 digit

Table A2. Induction motor.

Motor	Voltage (V)	Current (A)	Power (kW)	Power Factor	Speed (r/min)	Frequency (Hz)
DL1021 DeLorenzo (two poles)	220/380 (Δ/Y)	4.5/2.6 (Δ/Y)	1.1	0.85	2820	50

Table A3. Direct current generator.

DC Generator	Voltage (V)	Current (A)	Power (kW)
DL1024 DeLorenzo	220	3.4	0.75

Table A4. Frequency converter.

Frequency Converter	Power (kW)	Speed Range in Open-Loop Mode (Hz)	Voltage (V)
Telemecanique Altivar 71	0.75	1–100	200–240

Three different sets of magnets were used to fix the smartphone to the induction motor or to its supporting structure: (a) four magnets of 10 mm diameter, (b) one magnet of 40 mm diameter, and (c) one magnet of 40 mm diameter and two magnets of 10 mm diameter. Figure A1a shows the magnet of 40 mm, and Figure A1b shows four magnets of 10 mm.

(**a**)   (**b**)
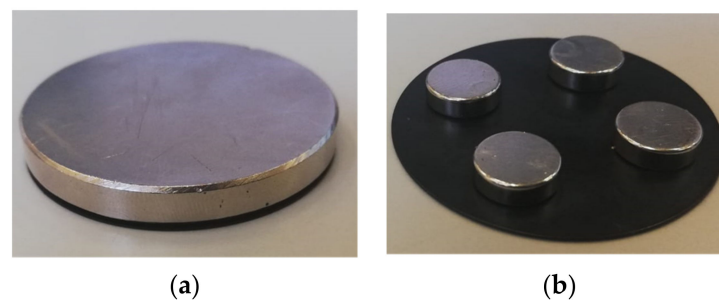
Figure A1. Sets of magnets: (**a**) magnet of 40 mm diameter; (**b**) four magnets of 10 mm diameter.

A basic smartphone, released in 2017, with the free application Physics Toolbox Sensor Suite from Vieyra Software [37], was used in the experimental section of this work.

References

1. Karlovský, P.; Lettl, J. Application of MRAS Algorithm to Replace the Speed Sensor in Induction Motor Drive System. *Procedia Eng.* **2017**, *192*, 421–426. [CrossRef]
2. Marfoli, A.; Di Nardo, M.; Degano, M.; Gerada, C.; Chen, W. Rotor Design Optimization of Squirrel Cage Induction Motor-Part I: Problem Statement. *IEEE Trans. Energy Convers.* **2021**, *36*, 1271–1279. [CrossRef]
3. Di Nardo, M.; Marfoli, A.; Degano, M.; Gerada, C.; Chen, W. Rotor Design Optimization of Squirrel Cage Induction Motor—Part II: Results Discussion. *IEEE Trans. Energy Convers.* **2021**, *36*, 1280–1288. [CrossRef]
4. Beleiu, H.G.; Maier, V.; Pavel, S.G.; Birou, I.; Pica, C.S.; Darab, P.C. Harmonics consequences on drive systems with induction motor. *Appl. Sci.* **2020**, *10*, 1528. [CrossRef]
5. Waide, P.; Brunner, C.U. *Energy-Efficiency Policy Opportunities for Electric Motor-Driven Systems*; International Energy Agency: Paris, France, 2011; Available online: https://iea.blob.core.windows.net/assets/d69b2a76-feb9-4a74-a921-2490a8fefcdf/EE_for_ElectricSystems.pdf (accessed on 2 February 2022).
6. Sousa-Santos, V.; Cabello-Eras, J.J.; Sagastume-Gutierrez, A.; Cabello-Ulloa, M.J. Assessment of the energy efficiency estimation methods on induction motors considering real-time monitoring. *Meas. J. Int. Meas. Confed.* **2019**, *136*, 237–247. [CrossRef]
7. Chirindo, M.; Khan, M.A.; Barendse, P. Analysis of Non-Intrusive Rotor Speed Estimation Techniques for Inverter-Fed Induction Motors. *IEEE Trans. Energy Convers.* **2021**, *36*, 338–347. [CrossRef]

8.   Salomon, C.P.; Sant'Ana, W.C.; Lambert-Torres, G.; Borges Da Silva, L.E.; Bonaldi, E.L.; De Oliveira, L.E.D.L. Comparison among methods for induction motor low-intrusive efficiency evaluation including a new AGT approach with a modified stator resistance. *Energies* **2018**, *11*, 691. [CrossRef]

9.   Zaky, M.S.; Khater, M.; Yasin, H.; Shokralla, S.S. Review of different speed estimation schemes for sensorlessinduction motor drives. *JEE* **2008**, *8*, 102–140.

10.   Alsofyani, I.M.; Idris, N.R.N. A review on sensorless techniques for sustainable reliablity and efficient variable frequency drives of induction motors. *Renew. Sustain. Energy Rev.* **2013**, *24*, 111–121. [CrossRef]

11.   Aiello, M.; Cataliotti, A.; Nuccio, S. An induction motor speed measurement method based on current harmonic analysis with the chirp-Z transform. *IEEE Trans. Instrum. Meas.* **2005**, *54*, 1811–1819. [CrossRef]

12.   Phumiphak, P.; Chat-uthai, C. Nonintrusive method for estimating field efficiency of inverter- fed induction motor using measured values. In Proceedings of the 2008 IEEE International Conference on Sustainable Energy Technologies, Singapore, 24–27 November 2008; pp. 580–583. [CrossRef]

13.   Rodopoulos, K.; Yiakopoulos, C.; Antoniadis, I. A parametric approach for the estimation of the instantaneous speed of rotating machinery. *Mechan. Syst. Signal Processing* **2014**, *44*, 31–46. [CrossRef]

14.   Rzeszucinski, P.; Lewandowski, D.; Pinto, C.T. Mobile device-based shaft speed estimation. *Measurement* **2017**, *96*, 52–57. [CrossRef]

15.   Combet, F.; Zimroz, R. A new method for the estimation of the instantaneous speed relative fluctuation in a vibration signal based on the short time scale transform. *Mechan. Syst. Signal Processing* **2009**, *23*, 1382–1397. [CrossRef]

16.   Wang, T.; Yan, Y.; Wang, L.; Hu, Y. Rotational speed measurement through image similarity evaluation and spectral analysis. *IEEE Access* **2018**, *6*, 46718–46730. [CrossRef]

17.   Ferreira, F.J.T.E.; Duarte, A.F.F.; Lopes, F.J.P. Experimental evaluation of a novel webcam-based tachometer for in-situ rotational speed measurement. *Proc. IEEE Int. Conf. Ind. Technol.* **2020**, *2020*, 917–924. [CrossRef]

18.   Da Silva, J.C.; de Vasconcelos Lima, T.L.; de Lucena Júnior, J.A.; Lyra, G.J.; Souto, F.V.; de Souza Pimentel, H.; Belo, F.A.; Filho, A.C.L. Non-invasive method for in-service induction motor efficiency estimation based on sound acquisition. *Appl. Sci.* **2020**, *10*, 3757. [CrossRef]

19.   Paramo-Balsa, P.; Roldan-Fernandez, J.M.; Burgos-Payan, M.; Riquelme-Santos, J.M. A Low-Cost Non-Intrusive Method for In-Field Motor Speed Measurement Based on a Smartphone. *Sensors* **2021**, *21*, 4317. [CrossRef]

20.   Asad, B.; Vaimann, T.; Belahcen, A.; Kallaste, A.; Rassõlkin, A.; Ghafarokhi, P.S.; Kudelina, K. Transient Modeling and Recovery of Non-Stationary Fault Signature for Condition Monitoring of Induction Motors. *Appl. Sci.* **2021**, *11*, 2806. [CrossRef]

21.   Meira, M.; Bossio, G.R.; Verucchi, C.J.; Ruschetti, C.R.; Bossio, J.M. Speed Estimation during the Starting Transient of Induction Motors. *IEEE Trans. Instrum. Meas.* **2021**, *70*, 9000108. [CrossRef]

22.   Meira, M.; Bossio, G.; Verucchi, C.; Ruschetti, C.; Bossio, J. A speed self-sensing method in starting of induction motors. In Proceedings of the 18th Workshop on Information Processing and Control (RPIC), Salvador, Brazil, 18–20 September 2019; pp. 53–58. [CrossRef]

23.   Song, X.; Wang, Z.; Li, S.; Hu, J. Sensorless Speed Estimation of an Inverter-fed Induction Motor Using the Supply Side Current. *IEEE Trans. Energy Convers.* **2018**, *34*, 1432–1441. [CrossRef]

24.   Jia, Z.; Sharma, A. Review on engine vibration fault analysis based on data mining. *J. Vibroeng.* **2021**, *23*, 1433–1445. [CrossRef]

25.   Jamal, M.R.; Al Rasheed, K.S. Vibration Measurement of a Rotating Shaft using Electrostatic Sensor. *Int. J. Recent Technol. Eng.* **2021**, *10*, 97–105. [CrossRef]

26.   Dlamini, V.; Naidoo, R.; Manyage, M. A non-intrusive method for estimating motor efficiency using vibration signature analysis. *Int. J. Electr. Power Energy Syst.* **2013**, *45*, 384–390. [CrossRef]

27.   Karlsson, R.; Hendeby, G. Speed Estimation From Vibrations Using a Deep Learning CNN Approach. *IEEE Sens. Lett.* **2021**, *5*, 7000504. [CrossRef]

28.   Dionisio, R.; Torres, P.; Ramalho, A.; Ferreira, R. Magnetoresistive sensors and piezoresistive accelerometers for vibration measurements: A comparative study. *J. Sens. Actuator Netw.* **2021**, *10*, 22. [CrossRef]

29.   Kalra, D. Overriding FINTECH. In Proceedings of the 2019 International Conference on Digitization (ICD), Sharjah, United Arab Emirates, 18–19 November 2019; pp. 254–259. [CrossRef]

30.   Krichen, M. Anomalies Detection through Smartphone Sensors: A Review. *IEEE Sens. J.* **2021**, *21*, 7207–7217. [CrossRef]

31.   Poulose, A.; Kim, J.; Han, D.S. A Sensor Fusion Framework for Indoor Localization Using Smartphone Sensors and Wi-Fi RSSI Measurements. *Appl. Sci.* **2019**, *9*, 4379. [CrossRef]

32.   Ashraf, I.; Hur, S.; Park, Y. Application of Deep Convolutional Neural Networks and Smartphone Sensors for Indoor Localization. *Appl. Sci.* **2019**, *9*, 2337. [CrossRef]

33.   Gutierrez-Martinez, J.-M.; Castillo-Martinez, A.; Medina-Merodio, J.-A.; Aguado-Delgado, J.; Martinez-Herraiz, J.-J. Smartphones as a Light Measurement Tool: Case of Study. *Appl. Sci.* **2017**, *7*, 616. [CrossRef]

34.   Cerrato-Alvarez, M.; Frutos-Puerto, S.; Arroyo, P.; Miró-Rodríguez, C.; Pinilla-Gil, E. A portable, low-cost, smartphone assisted methodology for on-site measurement of NO_2 levels in ambient air by selective chemical reactivity and digital image analysis. *Sens. Actuators B Chem.* **2021**, *338*, 129867. [CrossRef]

35.   Kalra, N.; Goyal, R.K.; Parashar, A.; Singh, J.; Singla, G. Driving Style Recognition System Using Smartphone Sensors Based on Fuzzy Logic. *Comput. Mater. Contin.* **2021**, *69*, 1967–1978. [CrossRef]

36. Nasr, M.; Islam, M.M.; Shehata, S.; Karray, F.; Quintana, Y. Smart Healthcare in the Age of AI: Recent Advances, Challenges, and Future Prospects. *IEEE Access* **2021**, *9*, 145248–145270. [CrossRef]

37. Vieyra Software. Physics Toolbox Sensor Suite (Version 7 August 2021) [Mobile Application]. Google Play Store. 2021. Available online: https://play.google.com/store/apps/details?id=com.chrystianvieyra.physicstoolboxsuite&hl=es_419&gl=US (accessed on 8 August 2021).

38. Heideman, M.; Johnson, D.; Burrus, C. Gauss and the history of the fast Fourier transform. *IEEE ASSP Mag.* **1984**, *1*, 14–21. [CrossRef]